RSC Advances

PAPER

View Article Online
View Journal | View Issue

Cite this: *RSC Adv.*, 2021, **11**, 22820

Synthesis of 2-methoxybenzamide derivatives and evaluation of their hedgehog signaling pathway inhibition†

Chiyu Sun, * Dajun Zhang, Tian Luan, Youbing Wang, Wenhu Zhang, Lin Lin, Meihua Jiang, Ziqian Hao and Ying Wang

Received 27th January 2021
Accepted 22nd June 2021

DOI: 10.1039/d1ra00732g

rsc.li/rsc-advances

Aberrant hedgehog (Hh) signaling is implicated in the development of a variety of cancers. Smoothened (Smo) protein is a bottleneck in the Hh signal transduction. The regulation of the Hh signaling pathway to target the Smo receptor is a practical approach for development of anticancer agents. We report herein the design and synthesis of a series of 2-methoxybenzamide derivatives as Hh signaling pathway inhibitors. The pharmacological data demonstrated that compound **21** possessed potent Hh pathway inhibition with a nanomolar IC_{50} value, and it prevented Shh-induced Smo from entering the primary cilium. Furthermore, mutant Smo was effectively suppressed *via* compound **21**. The *in vitro* antiproliferative activity of compound **21** against a drug-resistant cell line gave encouraging results.

Introduction

The hedgehog (Hh) signaling pathway is one of the pivotal targets for cancer therapy, and it is fundamental in regulating embryonic development and maintaining homeostasis of adult tissues.[1–4] Upon secretion of Hh ligands, the transmembrane protein patched (Ptch) abrogates its inhibition of smoothened (Smo) receptor.[5–8] Smo trafficking into the primary cilium (PC) transmits the signal to the downstream cascade.[9–11] The glioma (Gli) transcription factors translocate into the nucleus and activate the target genes.[12–14] Abnormal activation of the Hh pathway is able to facilitate tumorigenesis and metastasis, inducing multiple solid tumors and non-solid tumors such as basal cell carcinoma (BCC), medulloblastoma (MB), pancreatic carcinoma, colorectal carcinoma and leukaemia.[15–20] Hence, the inhibition of the Hh signaling pathway is deemed as a promising option for antitumor therapy.

There have been two highly efficacious Hh pathway inhibitors, vismodegib (**1**) and sonidegib (**2**) (Fig. 1), launched for treating BCC nowadays.[21–23] However, it was reported that 30 percent of patients who had taken **1** suffered from several adverse reactions such as muscle cramps, hair loss, taste disorders, weight loss, and fatigue.[24,25] Besides, acquired drug resistance is a major drawback with this class of drugs. The best studied instance was that Smo mutation (D473H) interfered with the binding of the drug to Smo.[26,27] Similarly, Smo D477G in the mouse MB allograft model was deemed as a comparable murine Smo mutant.[28,29] The bottlenecks of Hh pathway inhibitors have prompted an extensive search for novel chemotype inhibitor.

In recent years, several benzimidazole derivatives, such as glasdegib, SANT-2(**3**), have exhibited potent Hh pathway inhibition, all of which target Smo receptor.[30–32] Compound **3** is a known Smo inhibitor with submicromolar IC_{50} in the Shh light II test.[33] Combination of glasdegib and low-dose of arabinoside are currently for the treatment of leukemia.[34] Alternatively, aryl amide groups in some Hh antagonists were deemed as the pharmacophores responsible for high affinity with Smo receptor, for instance, taladegib, XL139 and MDB5.[35–37] In our effort on the discovery of novel chemotype Hh inhibitors (Fig. 2), aryl amide group was introduced into compound **3** to replace the metabolically labile triethoxy groups. The resulting compound **4** (IC_{50} of 0.25 μM) displayed similar potency to compound **3** in Gli-luciferase (Gli-luc) reporter assay. With the addition of methoxy, the formation of a new hydrogen bond (H-bond) acceptor was in compound **10** (IC_{50} of 0.17 μM). To enhance the molecular flexibility, the replacement of benzimidazole with phenyl imidazole fragment offered compound **17** with higher potency (IC_{50} of 0.12 μM) in the light of the ring-opening strategy. Followed by Smo crystal structures analysis (PDB ID: 5L7I),[38] compounds **3**, **4**, **10** and **17** were docked into

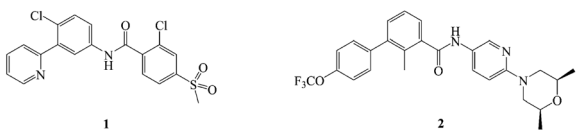

Fig. 1 Structure of hedgehog pathway inhibitors.

School of Pharmacy, Shenyang Medical College, Shenyang 110034, China. E-mail: scy_dream@126.com

† Electronic supplementary information (ESI) available. See DOI: 10.1039/d1ra00732g

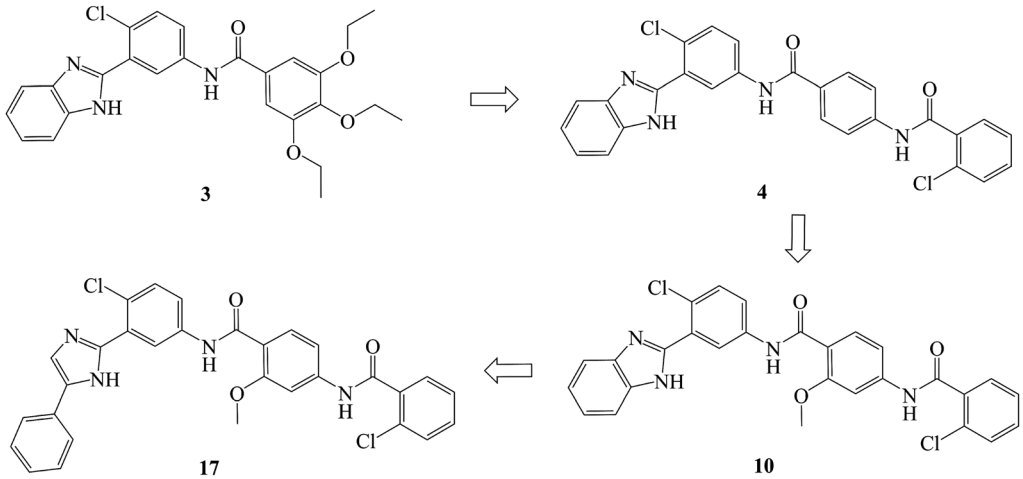

Fig. 2 Design of 2-methoxybenzamide derivatives.

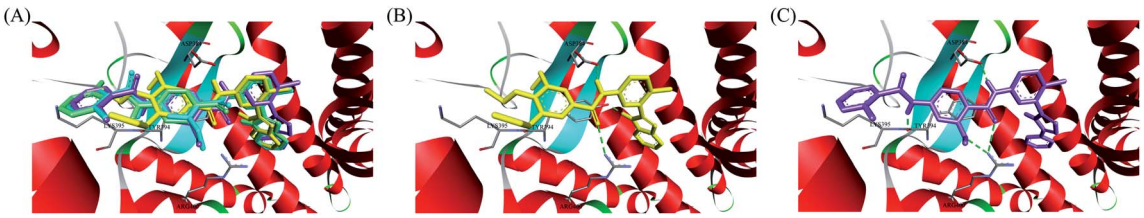

Fig. 3 (A) Overlay of compounds **3** (yellow), **4** (green), **10** (blue) and **17** (violet) in binding pocket of Smo. (B) Docking conformation of compound **3** at the binding site. (C) Docking conformation of compound **17** at the binding site. Hydrogen bonds are represented by the dashed green lines. Surrounding amino acid are shown in grey stick format and labelled.

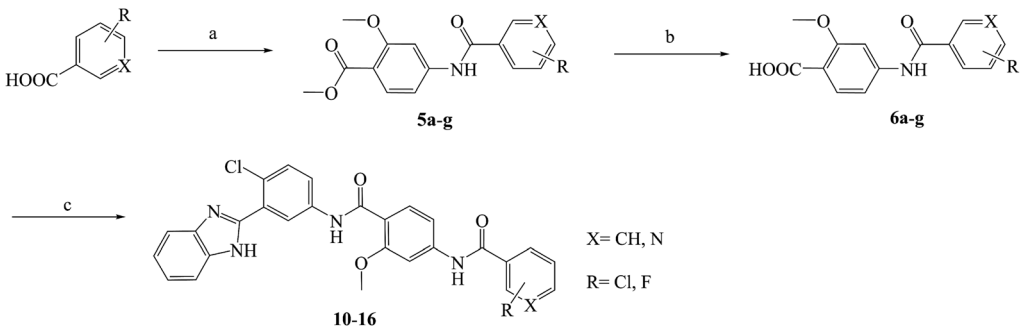

Scheme 1 Reagents and conditions: (a) (**1**) $SOCl_2$, toluene, 80 °C, 3 h; (**2**) methyl 4-amino-2-methoxybenzoate, TEA, DMF, rt, overnight, yield 85%; (b) NaOH, aqueous alcohol, 40 °C, 5 h, yield 83–92%; (c) 3-(1*H*-benzo[*d*]imidazol-2-yl)-4-chloroaniline, HATU, DIPEA, DCM, rt, 24 h, yield 71–86%; the specific position of R group directed at Table 1.

the binding pocket of Smo receptor using AutoDock vina.[39] The calculated binding energy of their best poses was −9.4, −10.9, −12.5, −12.7 kcal mol^{-1}, respectively, and their binding orientations superimposed well with one another (Fig. 3A). Comparing the interaction patterns between compounds **3** and **17** (Fig. 3B and C), the introduction of aryl amide group and methoxy afforded two extra H-bonds with Tyr394 and Arg400. Herein, the novel compounds with 2-methoxybenzamide skeleton were developed and their Hh pathway inhibition were evaluated.

Result and discussion

Chemistry

Compounds **10–23** were prepared according to the routes outlined in Schemes 1 and 2. Substituted acids refluxed in $SOCl_2$ for 3 h to generate acyl chlorides, which were condensed with methyl 4-amino-2-methoxybenzoate in the presence of triethylamine in dimethyl formamide at room temperature overnight to obtain the intermediate **5a–g**. Then, the esters were hydrolyzed to the carboxylic acid **6a–g**, before their amidation with 3-(1*H*-benzo[*d*]imidazol-2-yl)-4-chloroaniline[33] afforded the target

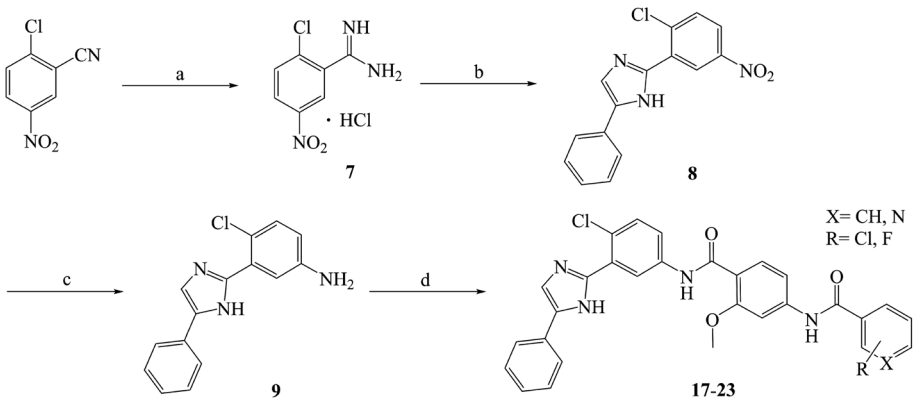

Scheme 2 Reagents and conditions: (a) CH_3ONa, CH_3OH, −20 °C, 2 h; NH_4Cl, 40 °C, 3 h, yield 46%; (b) 2-bromoacetophenone, $NaHCO_3$, THF, reflux, 40 °C, 24 h, yield 65%; (c) $SnCl_2 \cdot 2H_2O$, ethanol, HCl, 80 °C, reflux, 8 h, yield 86%; (d) **5a–g**, HATU, DIPEA, DCM, rt, 24 h, yield 76–84%; the specific position of R group directed at Table 1.

Table 1 Hh signaling pathway inhibition of designed compounds

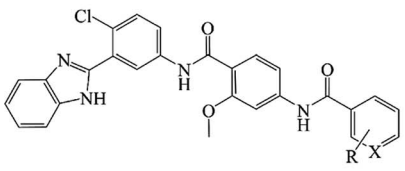

Compounds 10-16

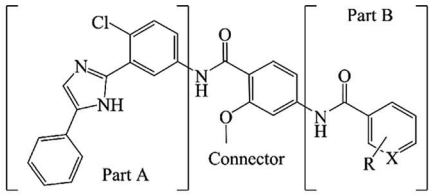

Compounds 17-23

Compd.	R	X	Yield (%)	Gli-luc reporter IC_{50}[a] (μM)
10	2-Cl	CH	75	0.17 ± 0.06
11	2,4-Cl_2	CH	71	0.53 ± 0.05
12	3-F	CH	83	0.79 ± 0.14
13	4-F	CH	85	0.34 ± 0.07
14	2-Cl	N	80	0.05 ± 0.02
15	6-Cl	N	73	0.86 ± 0.09
16	—	N	86	0.08 ± 0.02
17	2-Cl	CH	79	0.12 ± 0.06
18	2,4-Cl_2	CH	76	0.26 ± 0.08
19	3-F	CH	84	0.31 ± 0.09
20	4-F	CH	82	0.25 ± 0.04
21	2-Cl	N	81	0.03 ± 0.01
22	6-Cl	N	77	0.15 ± 0.08
23	—	N	83	0.07 ± 0.02
3[b]				0.18 ± 0.03
1[c]				0.02 ± 0.01

[a] Results expressed as the mean ± standard deviation of three separate IC_{50} determinations. For each determination, concentration-inhibition curves were acquired in triplicate and then averaged to afford a single IC_{50} curve with a 95% confidence interval. [b] Used as a lead compound. [c] Used as a positive control.

compounds **10–16**. In the presence of sodium alkoxide, 2-chloro-5-nitrobenzonitrile and ammonium chloride combined chemically to produce amidine hydrochloride **7** in a yield of 45%. Next, the cyclization of **7** and 2-bromoacetophenone gave imidazole intermediate **8**, which converted to amino compound **9** by adding stannous chloride in acidic ethanol solution. The condensation of **9** with **6a–g** generated the target compounds **17–23**.

Biological evaluation

As shown in Table 1, the targeted compounds contained the following three parts: A, B and a connector. Part A involved imidazole group, and part B contained aryl amide. 2-Methoxybenzamide scaffold was the connector.

Using compound **1** as positive control and compound **3** as the lead compound, the Hh pathway inhibition of compounds

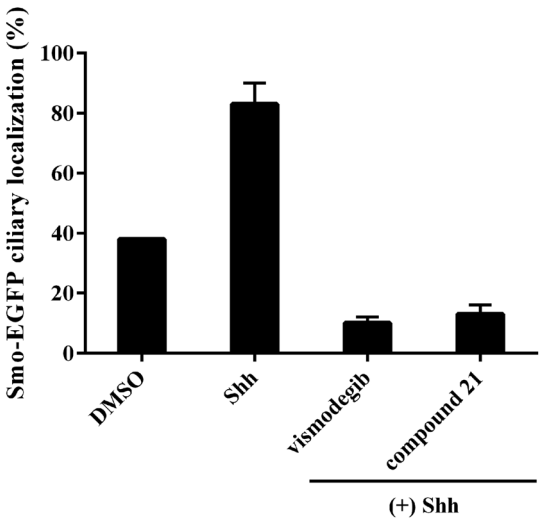

Fig. 4 Benzamide analogs inhibit Hh pathway through regulating Smo. Error bars represent standard deviation of three parallel groups.

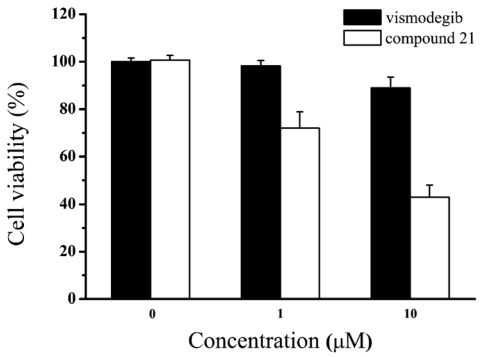

Fig. 6 Cell viability of Daoy cells incubated with the indicated doses of vismodegib and compound **21** for 48 h. Data represent mean ± SD of experiments performed in triplicate.

10–23 have been evaluated in Gli luciferase reporter assay. The results were expressed as IC_{50} values. At the outset, the relationship between part A and its Hh inhibitory activity was discussed. Encouragingly, the activity of phenyl imidazole analogues were higher than that of benzimidazole counterparts (**11** *vs.* **18**, **12** *vs.* **19** and **13** *vs.* **20**), suggesting that ring-opening structural modification was effective. Further analysis revealed that different Hh pathway inhibition was observed as various R groups were introduced into the aromatic ring (part B). Monochlorine substituent **17** exhibited decent activity (IC_{50} = 0.12 μM), however, dichloride **18** lost potency by 2.2-fold (IC_{50} = 0.26 μM). Although fluoro analogs such as **19** and **20** (IC_{50} = 0.31 μM and 0.25 μM) were effective in suppressing Hh signaling pathway, their IC_{50} values were larger than that of compound **17**. We then enhanced the hydrophilicity of part B by replacing phenyl with pyridine, and it was satisfying that the potency of pyridyl derivative **21** (IC_{50} = 0.03 μM) was higher as compared to that of phenyl derivative **17**. When chlorine located at 2′-position of nicotinamide group, its anti-Hh activity improved (**21** *vs.* **23** and **14** *vs.* **16**). Diminished activity was observed as the chlorine transferred to the 6′-position of the nicotinamide group (**22** *vs.* **23**). Overall, compound **21** yielded the most potent activity in this class, which was even 6-fold higher as compared to compound **3**. Also, the Hh pathway inhibition of compound **21** was comparable to that of compound **1**.

To explore the mode of action of the representative compound **21** in Hh signaling pathway, its effect on Smo ciliary translocation was measured. As presented in Fig. 4, Smo localization in the primary cilia enhanced significantly as the NIH3T3 cells expressing Smo were treated with Shh, an agonist of Hh pathway. In compound **21** group, there was a sharp drop in Smo ciliary translocation, and this result was similar to that of vismodegib group, indicating that the target of compound **21** was Smo receptor. It was reported that drug-resistant mutation in Smo reduced the Hh pathway inhibition of vismodegib by a large of margin.[40] To further test the potency of compound **21** on Smo mutation, wild-type (WT) or mutant D477G was overexpressed in the NIH3T3-Gli-Luc reporter cell line. Compliant with previous reports, mutant D477G was refractory to vismodegib (Fig. 5A). In contrast, the Hh pathway inhibitory activity of compound **21** slightly decreased in mutant D477G (Fig. 5B). The 2.4-fold shift in IC_{50} suggested that mutant D477G did not markedly influence its interaction with Smo (IC_{50} = 39 nM for WT, IC_{50} = 96 nM for mutant).

Due to the failure of vismodegib to kill MB cells in patient,[41] it was anticipated that compound **21** obtained a positive respond *in vitro*. Then, we carried out the antiproliferative assay

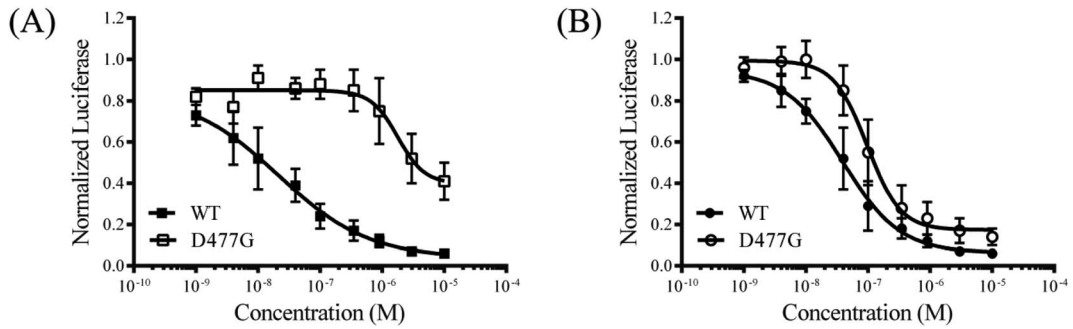

Fig. 5 The inhibition of drug-resistant Smo mutant for compound **21**. The inhibition of Gli-Luc reporter activity by vismodegib (A) and compound **21** (B) in NIH3T3-Gli-Luc cells overexpressing wild-type Smo or Smo D477G. Error data point represents the mean ± SD of three determinations.

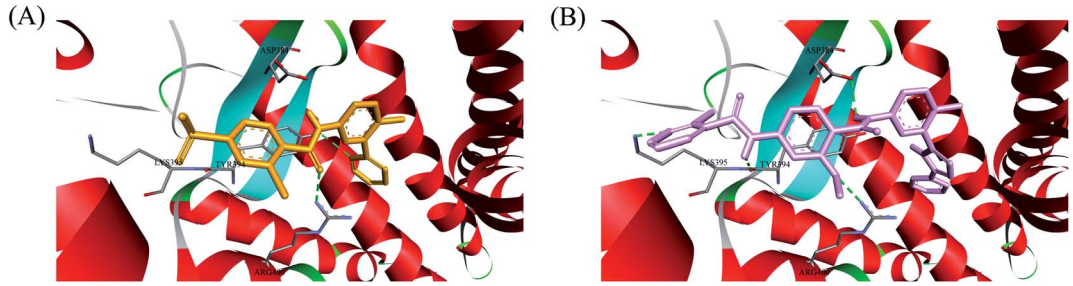

Fig. 7 (A) Docking conformation of compound **1** (orange) at the binding site. (B) Docking conformation of compound **21** (pink) at the binding site. Hydrogen bonds are represented by the dashed green lines. Surrounding amino acid are shown in grey stick format and labelled.

on Daoy cell line which was a proper MB model with consecutive Hh signaling activation. To our delight, compared with vismodegib, compound **21** demonstrated stronger antiproliferation against Daoy cells (Fig. 6). And the cell viabilities of compound **21** were 72% and 43% at concentrations of 1 μM and 10 μM, respectively.

In order to investigate the binding mode of this series of compounds with Smo receptor, a complete molecular docking study was carried out. As presented in Fig. 7A, compound **1** bound with Smo by H-bonds that contained the carbonyl moiety interacting with residue Arg400 and the nitrogen atom of pyridine interacting with residue Tyr394. Additionally, compound **21** kept tight interaction with residues Asp384, Tyr394, Lys395 and Arg400 (Fig. 7B), which showed two more binding sites in comparison with compound **1**. The computational modeling study interpreted the better Hh pathway inhibition of compound **21** at the molecular level.

Conclusions

In this report, novel series of Hh signaling pathway antagonists with 2-methoxybenzamide skeleton were explored by structural modification based on SANT-2. In Gli-luc reporter assay, this class of inhibitors entirely showed submicromolar range of IC_{50} value, signifying that the 2-methoxybenzamide scaffold as connector was advantageous to their Hh pathway inhibition. Thereinto, the IC_{50} value of compound **21** was 0.03 μM, and the molecular basis of its inhibition was ascribed to the blockade of Smo. Especially, compound **21** retained the suppressive potency against mutant and WT Smo, moreover, it displayed better antiproliferative activity against vismodegib-resistant Daoy cells. Further structural optimization is currently in progress and will be reported in due course.

Conflicts of interest

There are no conflicts to declare.

Acknowledgements

This work was supported financially by the National Natural Science Foundation of China (82003656), Liaoning Science and Technology Project Management (2020-MS-313), the Science and Technology Fund Project of Shenyang Medical College (20201004 and 20205041).

Notes and references

1 H. J. Sharpe, W. R. Wang, R. N. Hannoush and F. J. de Sauvage, *Nat. Chem. Biol.*, 2015, **11**, 246–255.
2 I. Galperin, L. Dempwolff, W. E. Diederich and M. Lauth, *J. Med. Chem.*, 2019, **62**, 8392–8411.
3 A. E. Owens, I. D. Paola, W. A. Hansen, Y. W. Liu, S. D. Khare and R. Fasan, *J. Am. Chem. Soc.*, 2017, **139**, 12559–12568.
4 M. H. Xin, X. Y. Ji, L. K. D. L. Cruz, S. Thareja and B. H. Wang, *Med. Res. Rev.*, 2018, **38**, 870–913.
5 A. Salaritabar, I. Berindan-Neagoe, B. Darvish, F. Hadjiakhoondi, A. Manayi, K. P. Devi, D. Barreca, I. E. Orhan, I. Suntar, A. A. Farooqi, D. Gulei, S. F. Nabavi, A. Sureda, M. Daglia, A. R. Dehpour, S. M. Nabavi and S. Shirooie, *Pharmacol. Res.*, 2019, **141**, 466–480.
6 I. Deshpande, J. H. Liang, D. Hedeen, K. J. Roberts, Y. X. Zhang, B. Ha, N. R. Latorraca, B. Faust, R. O. Dror, P. A. Beachy, B. R. Myers and A. Manglik, *Nature*, 2019, **571**, 284–288.
7 J. E. Cortes, R. Gutzmer, M. W. Kieran and J. A. Solomon, *Cancer Treat. Rev.*, 2019, **76**, 41–50.
8 H. Farrokhpour, V. Pakatchian, A. Hajipour, F. Abyar, A. N. Chermahini and F. Fakhari, *RSC Adv.*, 2015, **5**, 68829–68838.
9 J. Kim, E. Y. C. Hsia, A. Brigui, A. Plessis, P. A. Beachy and X. Y. Zheng, *Sci. Signaling*, 2015, **8**, ra55.
10 D. Bhattarai, J. H. Jung, S. Han, H. Lee, S. J. Oh, H. W. Ko and K. Lee, *Eur. J. Med. Chem.*, 2017, **125**, 1036–1050.
11 A. M. Arensdorf, M. E. Dillard, J. M. Menke, M. W. Frank, C. O. Rock and S. K. Ogden, *Cell Rep.*, 2017, **19**, 2074–2087.
12 D. Z. Ji, W. W. Zhang, Y. G. Xu and J. J. Zhang, *Bioorg. Med. Chem.*, 2020, **28**, 115354.
13 T. N. Trinh, E. A. McLaughlin, C. P. Gordon, I. R. Bernstein, V. J. Pye, K. A. Redgrove and A. McCluskey, *Org. Biomol. Chem.*, 2017, **15**, 3046–3059.
14 Y. Wang, A. C. Arvanites, L. Davidow, J. Blanchard, K. Lam, J. W. Yoo, S. Coy, L. L. Rubin and A. P. McMahon, *ACS Chem. Biol.*, 2012, **7**, 1040–1048.
15 E. Y. Lee, H. K. Ji, Z. Q. Ouyang, B. Y. Zhou, W. X. Ma, S. A. Vokes, A. P. McMahon, W. H. Wong and M. P. Scott, *Proc. Natl. Acad. Sci. U. S. A.*, 2010, **107**, 9736–9741.

16 B. Biehs, G. J. P. Dijkgraaf, R. Piskol, B. Alicke, S. Boumahdi, F. Peale, S. E. Gould and F. J. de Sauvage, *Nature*, 2018, **562**, 429–433.
17 S. M. Waszak, G. W. Robinson, B. L. Gudenas, K. S. Smith, A. Forget, M. Kojic, J. Garcia-Lopez, J. Hadley, K. V. Hamilton, E. Indersie, I. Buchhalter, J. Kerssemakers, N. Jäger, T. Sharma, T. Rausch, M. Kool, D. Sturm, D. T. W. Jones, A. Vasilyeva, R. G. Tatevossian, G. Neale, B. Lombard, D. Loew, J. Nakitandwe, M. Rusch, D. C. Bowers, A. Bendel, S. Partap, M. Chintagumpala, J. Crawford, N. G. Gottardo, A. Smith, C. Dufour, S. Rutkowski, T. Eggen, F. Wesenberg, K. Kjaerheim, M. Feychting, B. Lannering, J. Schüz, C. Johansen, T. V. Andersen, M. Röösli, C. E. Kuehni, M. Grotzer, M. Remke, S. Puget, K. W. Pajtler, T. Milde, O. Witt, M. Ryzhova, A. Korshunov, B. A. Orr, D. W. Ellison, L. Brugieres, P. Lichter, K. E. Nichols, A. Gajjar, B. J. Wainwright, O. Ayrault, J. O. Korbel, P. A. Northcott and S. M. Pfister, *Nature*, 2020, **580**, 396–401.
18 V. Kumar, G. Mondal, P. Slavik, S. Rachagani, S. K. Batra and R. I. Mahato, *Mol. Pharmaceutics*, 2015, **12**, 1289–1298.
19 L. Vesci, F. M. Milazzo, M. A. Stasi, S. Pace, F. Manera, C. Tallarico, E. Cini, E. Petricci, F. Manetti, R. D. Santis and G. Giannin, *Eur. J. Med. Chem.*, 2018, **157**, 368–379.
20 C. Zhao, A. Chen, C. H. Jamieson, M. Fereshteh, A. Abrahamsson, J. Blum, H. Y. Kwon, J. Kim, J. P. Chute, D. Rizzieri, M. Munchhof, T. VanArsdale, P. A. Beachy and T. Reya, *Nature*, 2009, **458**, 776–779.
21 M. Wahid, A. Jawed, R. K. Mandal, S. A. Dar, S. Khan, N. Akhter and S. Haque, *Critical Reviews in Oncology/Hematology*, 2016, **98**, 235–241.
22 A. M. Giannetti, H. Wong, G. J. P. Dijkgraaf, E. C. Dueber, D. F. Ortwine, B. J. Bravo, S. E. Gould, E. G. Plise, B. L. Lum, V. Malhi and R. A. Graham, *J. Med. Chem.*, 2011, **54**, 2592–2601.
23 S. Jain, R. L. Song and J. W. Xie, *OncoTargets Ther.*, 2017, **10**, 1645–1653.
24 A. Kumari, A. N. Ermilov, M. Grachtchouk, A. A. Dlugosz, B. L. Allen, R. M. Bradley and C. M. Mistretta, *Proc. Natl. Acad. Sci. U. S. A.*, 2017, **114**, 10369–10378.
25 F. Ghirga, M. Mori and P. Infante, *Bioorg. Med. Chem. Lett.*, 2018, **28**, 3131–3140.
26 S. X. Atwood, K. Y. Sarin, R. J. Whitson, J. R. Li, G. Kim, M. Rezaee, M. S. Ally, J. Kim, C. Yao, A. L. S. Chang, A. E. Oro and J. Y. Tang, *Cancer Cell*, 2015, **27**, 342–353.
27 X. C. Dong, C. L. Wang, Z. J. Chen and W. L. Zhao, *Drug Discovery Today*, 2018, **23**, 704–710.
28 S. Coni, P. Infante and A. Gulino, *Biochem. Pharmacol.*, 2013, **85**, 623–628.
29 H. Y. Tao, Q. H. Jin, D. Koo, X. B. Liao, N. P. Englund, Y. Wang, A. Ramamurthy, P. G. Schultz, M. Dorsch, J. Kelleher and X. Wu, *Chem. Biol.*, 2011, **18**, 432–437.
30 P. L. Bedard, D. M. Hyman, M. S. Davids and L. L. Siu, *Lancet*, 2020, **395**, 1078–1088.
31 M. J. Munchhof, Q. F. Li, A. Shavnya, G. V. Borzillo, T. L. Boyden, C. S. Jones, S. D. LaGreca, L. Martinez-Alsina, N. Patel, K. Pelletier, L. A. Reiter, M. D. Robbins and G. T. Tkalcevic, *ACS Med. Chem. Lett.*, 2012, **3**, 106–111.
32 J. K. Chen, J. Taipale, K. E. Young, T. Maiti and P. A. Beachy, *Proc. Natl. Acad. Sci. U. S. A.*, 2002, **99**, 14071–14076.
33 A. Büttner, K. Seifert, T. Cottin, V. Sarli, L. Tzagkaroulaki, S. Scholz and A. Giannis, *Bioorg. Med. Chem.*, 2009, **17**, 4943–4954.
34 J. E. Cortes, F. H. Heidel, A. Hellmann, W. Fiedler, B. D. Smith, T. Robak, P. Montesinos, D. A. Pollyea, P. DesJardins, O. Ottmann, W. W. Ma, M. N. Shaik, A. D. Laird, M. Zeremski, A. O'Connell, G. Chan and M. Heuser, *Leukemia*, 2019, **33**, 379–389.
35 C. Wang, H. X. Wu, V. Katritch, G. W. Han, X. P. Huang, W. Liu, F. Y. Siu, B. L. Roth, V. Cherezov and R. C. Stevens, *Nature*, 2013, **497**, 338–343.
36 M. R. Tremblay, M. Nesler, R. Weatherhead and A. C Castro, *Expert Opin. Ther. Pat.*, 2009, **19**, 1039–1056.
37 V. Kumar, A. K. Chaudhary, Y. X. Dong, H. A. Zhong, G. Mondal, F. Lin, V. Kumar and R. I. Mahato, *Sci. Rep.*, 2017, **7**, 1665.
38 E. F. Byrne, R. Sircar, P. S. Miller, G. Hedger, G. Luchetti, S. Nachtergaele, M. D. Tully, L. Mydock-McGrane, D. F. Covey, R. P. Rambo, M. S. Sansom, S. Newstead, R. Rohatgi and C. Siebold, *Nature*, 2016, **535**, 517–522.
39 O. Trott and A. J. Olson, *J. Comput. Chem.*, 2010, **31**, 455–461.
40 S. Ohshima-Hosoyama, M. A. Davare, T. Hosoyama, L. D. Nelon and C. Keller, *J. Neuro-Oncol.*, 2011, **105**, 475–483.
41 R. L. Yauch, G. J. Dijkgraaf, B. Alicke, T. Januario, C. P. Ahn, T. Holcomb, K. Pujara, J. Stinson, C. A. Callahan, T. Tang, J. F. Bazan, Z. Kan, S. Seshagiri, C. L. Hann, S. E. Gould, J. A. Low, C. M. Rudin and F. J. de Sauvage, *Science*, 2009, **326**, 572–574.